particles

MDPI

Article

Concept of Isomer Beam Production with Heavy-Ion Storage Rings

Takayuki Yamaguchi [1,*], Yoshitaka Yamaguchi [2], Tetsuya Ohnishi [2], Daisuke Nagae [1] and Yury A. Litvinov [3,4]

[1] Department of Physics, Saitama University, Saitama 338-8570, Japan
[2] RIKEN Nishina Center, Wako 351-0198, Japan
[3] GSI Helmholtzzentrum für Schwerionenforschung, 64291 Darmstadt, Germany; y.litvinov@gsi.de
[4] Institut für Kernphysik, Universität zu Köln, 50937 Köln, Germany
* Correspondence: yamaguti@mail.saitama-u.ac.jp

Abstract

Heavy radioactive ion beams produced by in-flight techniques often involve long-lived excited states (isomers). This presents a challenge for reaction studies because none of the existing fragment separators worldwide can resolve isomers in-flight. Here, we propose a novel scheme to produce tagged cocktail beams or pure isomer beams using an ion storage ring. The mass resolving powers of storage rings enable us to identify and separate ions of the isomeric state from the corresponding ground state in a secondary beam. For short-lived isomers, the Rare-RI Ring (R3) facility at the RI Beam Factory (RIBF) will be available, while for long-lived isomers the Experimental Storage Ring (ESR) at the GSI/FAIR facility will be utilized. Isomers often have spins and deformations significantly different from the ground states. Studying isomer structures will provide unique insight into their specific interactions, opening a new frontier in reaction studies with radioactive ion beams in the coming years.

Keywords: in-flight fragment separators; ion storage rings; isomer beams

1. Introduction

Today heavy-ion storage rings are unique and versatile instruments for atomic and nuclear physics experiments [1]. Originally, storage rings were thought to accumulate stored ions to increase reaction luminosities, whereas meanwhile they are widely used to store highly charged radioactive ions for otherwise impossible experiments. Currently, there exist three operational storage ring facilities worldwide, which can store radioactive ions, namely the medium-energy Experimental Storage Ring (ESR) [2] coupled to a low-energy CRYRING [3] at GSI/FAIR , Cooler Storage Ring for experiments (CSRe) [4] at the Institute of Modern Physics (IMP), and Rare-RI Ring (R3) [5] at the RI Beam Factory (RIBF). It is emphasized that the Spectroscopy Storage Ring (SRing) [6] is being commissioned right now at the HIAF facility [7].

The greatest achievements of storage-ring nuclear physics programs have been mass and lifetime measurements of exotic nuclei [8]. There are two established mass spectrometry techniques [9]; Schottky mass spectrometry (SMS) for long-lived nuclei and isochronous mass spectrometry (IMS) for short-lived nuclei.

In general, radioactive ion beams produced by nuclear reaction inevitably have substantial momentum spreads. SMS employs the lengthy (in our present context) cooling

Check for updates

Academic Editors: Bing Guo, Baohua Sun, Yingxun Zhang, Pengwei Zhao and Qiang Zhao

Received: 11 February 2026
Revised: 16 March 2026
Accepted: 20 March 2026
Published: 29 March 2026

Copyright: © 2026 by the authors. Licensee MDPI, Basel, Switzerland. This article is an open access article distributed under the terms and conditions of the Creative Commons Attribution (CC BY) license.

techniques such as stochastic [10] and/or electron [11] cooling for all the stored ions to have the same velocity in the ring. This makes the revolution frequencies proportional to their mass-to-charge ratios only, thereby allowing broadband measurements of known and unknown masses at the same time [12,13]. Non-destructive Schottky detectors have been developed to measure revolution frequencies [14,15]. In the mean time, a mass resolving power of 10^6 is routinely achieved. Time-dependent monitoring of intensities of revolution frequency peaks provides effective lifetimes of stored ions, which can dramatically change in a high atomic charge state [16,17]. For example, fully stripped ^{205}Tl ions become radioactive, whereas neutral ones are stable on earth. Recently, the half-life of ^{205}Tl bound-state β decay was measured at ESR, which has provided new knowledge on the *s*-process nucleosynthesis [18] and feasibility to measure long-time averaged solar neutrino flux [19].

In general, IMS applies the isochronous optical condition to the ring lattice that cancels the velocity spread of each stored ion species so as to achieve the same revolution time in each turn. This also makes the revolution times only depend on the mass-to-charge ratios, enabling fast and precise mass measurements of exotic nuclei. Ultra-thin foil-based time-of-flight (TOF) detectors installed in a ring vacuum are routinely used to measure revolution times of stored ions [20]. Recently, the highest precision mass spectrometry termed $B\rho$-IMS has been realized utilizing two TOF detectors for in-ring velocity measurement at CSRe, where an order of 10 keV could be achieved [21–23].

Today, the ion storage rings are successfully employed to address nuclear reactions, such as direct (p, γ) and (p, n) for astrophysical p-process [24,25] or using surrogate approach to deduce neutron-induced cross-sections [26,27]. The ESR is equipped with multi-functions beam manipulation techniques that allow a unique environment to study such reactions in the inverse kinematics with an internal, windowless, ultra pure gas-jet target [28]. A loss of luminosities due to a small target density is compensated by the high revolution frequency of stored ions. The ability to decelerate stored beams utilizing radio-frequency (RF) cavities is key to investigate reactions of astrophysical relevance [29]. Beam accumulation through stacking and cooling cycles is decisive to increase the intensities of rarely-produced nuclei. Recently, the low-energy proton capture reaction with–for the first time–radioactive ^{118}Te has been successfully performed [30]. The ESR can store beams with energies as low as a few MeV/nucleon. To access stored beams with lower energies, a dedicated storage ring CRYRING [3] was rebuilt behind the ESR and is now ready to receive low-energy radioactive ions prepared at the FRS [31]–ESR facility. A campaign addressing astrophysical reactions is ongoing at the CRYRING with a dedicated setup CARME [32–34].

The achieved technologies of storage rings have several advantages compared to in-flight fragment separators. In particular, the mass resolving powers are approaching 10^6, which makes possible in-flight identification of isomeric states contained in secondary beams without γ-ray detection. In the following sections, a brief overview of fragment separators and ion storage rings is given followed by two methods proposed for isomer identification and separation. Finally, a few physics cases are introduced related to investigations of halo and skin structures of exotic nuclei.

2. Fragment Separators and Storage Rings

2.1. Conventional Fragment Separators

In-flight fragment separators are essential to secondary beam experiments. Forty years ago, the first halo nuclei were discovered for neutron-rich He and Li isotopes at the secondary beam line with the heavy ion spectrometer system HISS at the Lawrence Berkeley Laboratory [35,36]. High-energy interaction cross sections are an excellent probe to figure out the spatial distributions of nucleon densities of exotic nuclei. A nucleus with a

larger radius has larger geometrical overlap with a target nucleus in the collision, leading to a larger reaction probability. Glauber theory is typically used to reproduce the cross sections [37], where a density distribution of the projectile is implemented as a free fitting parameter, thus constraining the radius.

After the technical establishment of magnetic rigidity separation with energy loss analysis [38], the second-generation fragment separators such as FRS [31] at GSI, A1900 [39] at the National Superconducting Cyclotron Laboratory in Michigan, RIBLL2 [40] at IMP in Lanzhou and others were built worldwide and have blossomed radioactive ion beam science.

Today, the third-generation fragment separator BigRIPS at RIBF [41] and those upcoming at FRIB [42], HIAF [43], FAIR [44], and elsewhere commonly have a two-stage architecture for ever higher purification power as required for higher intensity primary beams: a pre-separator utilizing conventional methodology and a high-resolution main separator with the goal to identify every incoming particle before delivering it to an experimental station downstream. For example, the BigRIPS is currently providing the highest intensities of radioactive ion beams, e.g., halo nuclei ^{11}Li with 10^5 particles/s [45].

Three radioactive ion beam facilities have the storage ring branches: FRS-ESR at GSI, RIBLL2-CSRe at IMP, and BigRIPS-R3 at RIBF. The former two are synchrotron-based and the latter one is cyclotron-based facilities. The now-starting HIAF facility is also synchrotron based.

2.2. Storage Ring Technology for Radioactive Ion Beams

The advanced functions of heavy-ion storage rings are addressed; Injected ions are stored for an extended time period in an ultra high vacuum (UHV) environment. Because magnetic rigidity $B\rho$ of the ring is fixed, the stored ions have a specific atomic charge state Q, which can be selectively chosen to be fully stripped of electrons (bare nucleus), hydrogen-like ion with a single bound electron, or any other few-electron ion. Internal gas-jet target can be used as an electron target to strip off or capture electrons in the beam ions, or be used as a nuclear reaction target. Thus, unique studies on the interactions between electrons and nucleus are realized [46,47].

To increase the phase space density of stored ions, cooling techniques are employed; electron cooling, stochastic cooling, laser cooling, etc. The orbits of the stored ions are precisely tuned within the acceptance by applying proper RF fields. The beam energies can be decreased or increased by employing acceleration cavities. Depending on production yields and operation modes of the fragment separator, ion intensities can be as large as 10^6 particles or be just single ions injected and stored at each cycle, which may include either a single or multiple species in a coasting or bunched beam. Thus, beams of specific ion species and their emittances are precisely under control.

The exceptional feature is represented by mass resolving powers. In SMS, the electron cooling technique allows one to achieve momentum spreads as small as $\delta p/p \approx 10^{-7}$ when the number of stored ions is less than $n \lesssim 10^3$ [48]. The resolving power of SMS generally decreases with the increasing number of stored ions, whereas that of IMS depends only on the quality of the isochronous setting. Recently, an updated ring optics led to an improved mass resolving power approaching $\approx 10^6$, thereby enabling identification of low-lying isomers with excitation energy of only 100 keV [49].

Note, that a machine acceptance reflects secondary beam intensities and is thus a key characteristics of the fragment separators, whereas the mass resolving power is a key characteristics of the storage rings. Therefore, the facilities combining fragment separators and storage rings work–in principle–complementarily to provide highly intense and precisely resolved radioactive ion beams.

3. New Schemes of Isomer Beam Production

This section addresses the production of isomer beams at the facilities comprising a storage ring coupled to a fragment separator.

3.1. Short-Lived Isomers at R3

For short-lived nuclei, the Rare-RI Ring facility (R3) at RIBF will be available to produce isomer beams. As a premise, short-lived nuclei cannot be stored for a long time. They will decay within a short time even if injected and stored. That is the reason why the event-by-event injection scheme of R3 using the highest intensity beams from cyclotron is optimal. The latest status and details of R3 are covered in Ref. [50] and therein. Here, the working principle is briefly summarized. Figure 1 (top) schematically shows the BigRIPS and R3 beamline.

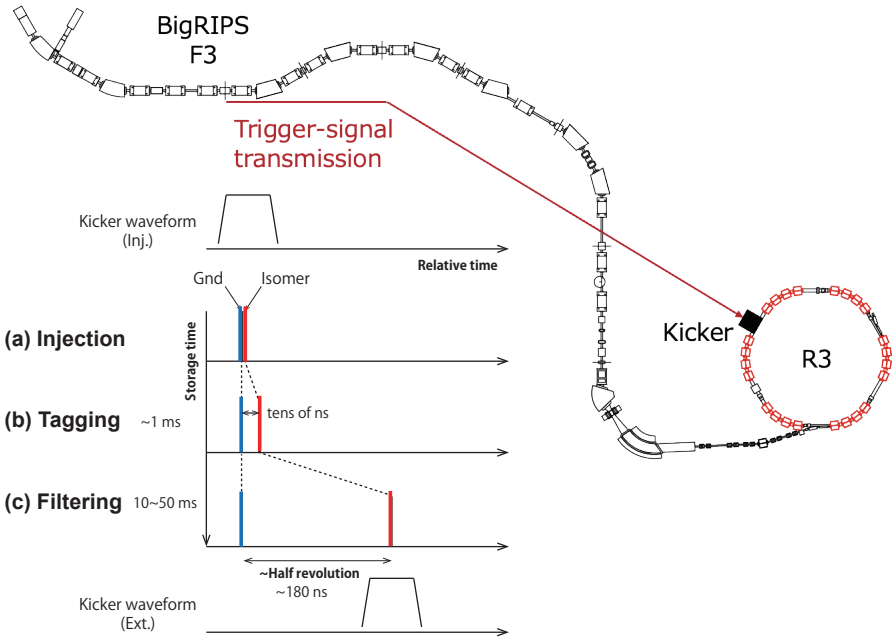


Figure 1. (**Top**) The BigRIPS and R3 beamline. Trigger signals at the F3 focal plane are transmitted to the kicker magnet of R3 for individual injection. (**Bottom**) Schematic of the isomer beam production in R3. Evolution of time differences between ions in the ground and isomeric states passing a specific place in the ring, e.g., the kicker magnet. (**a**) A single ion in either the ground or in the isomeric state is injected. (**b**) Tagging mode after ∼1 ms storage is essentially the same as a typical mass measurement, where the time difference is tens of ns, depending on the excitation energy. (**c**) Filtering mode for a pure isomer beam after a storage time of longer than 10 ms. The time difference becomes half of the revolution time, corresponding to ∼180 ns for 180 MeV/nucleon beams.

3.1.1. R3 Operation

Radioactive ions are produced by projectile fragmentation or in-flight fission reaction. Relativistic fragments are identified at the third focal plane (F3) of BigRIPS, where trigger signals are generated to excite the R3 kicker magnet. The identified ions within the R3 acceptance are injected one-by-one with 100 Hz (max.) kicker repetition. Note, that the applied pulsed magnetic field should be exactly synchronized with the ion arrival to the kicker position through a long beamline. This synchronization scheme, termed individual injection, has been successfully done by dedicated fast kicker system. An injected ion revolves approximately 2000 turns, corresponding to ∼1 ms storage time, before it is ejected by the same kicker magnet. The next ion to be injected should arrive

after the extraction of the circulating ion in the preceding cycle. Thus, the operation cycle comprising identification, injection, storage, and ejection is sequentially repeated in the particle-by-particle manner. Additional time-of-flight (TOF) and ΔE gate technique at F3 can further restrict the number of ion species to be injected (down to a single one), otherwise many reaction products are randomly injected depending on their yield ratios. For mass spectrometry, several species including reference nuclei with well-known masses and target nuclei with yet unknown masses should be measured in the same setting [51,52]. Assuming a precise isochronous condition, the revolution time of a stored ion is proportional to the mass-to-charge ratio, enabling single-ion mass spectrometry of exotic nuclei [53].

Isomers are simultaneously populated with other fragments with inherent probabilities at the production stage. They have the same A, Z, and Q with their corresponding ground states and the excitation energies are generally too small to be identified in-flight at BigRIPS. The TOF and ΔE technique at F3 should be always employed so that an injected ion is in either the ground state or an isomeric state of one specific nuclear species. The identification and separation are performed inside the storage ring, where the isochronous condition is tuned to the target nucleus to achieve the maximum mass resolving power. Two operation modes shown in Figure 1 (bottom) are proposed as follows.

3.1.2. Tagged Beam Mode

This mode is essentially the same as the standard mass measurement mode, but with an exception that only one target nuclear species (in the ground or isomeric state) is injected as shown in Figure 1a. In a case that half-lives of nuclei of interest are very short, of an order of several milliseconds or even less, storage times cannot be significantly extended and should remain the same as implemented in mass measurements. The recharge time of the kicker magnet limits the minimum storage time to be 0.7 ms, corresponding to approximately 2000 turns. Currently, the degree of isochronicity at R3 is $\sigma(D_{iso}) \approx 3$ ppm.

The time difference between an isomeric state and the ground state, ΔT, is proportional to the isomer excitation energy, E_x, (i.e., mass difference) and storage time, T_s, and is empirically expressed as $\Delta T(\mathrm{ns}) \approx \frac{0.72}{A^{0.99}} T_s(\mathrm{ms}) E_x(\mathrm{keV})$ at the beam energy of 180 MeV/nucleon. To be able to resolve isomeric states, the time difference ΔT should be larger than the intrinsic time spread caused from the isochronicity as $\Delta T \geq T_s D_{iso}$. This gives $E_x > 800$ keV (2σ) at $A \approx 100$ nuclei.

After $\sim$1 ms storage time, the ground and isomeric states are well separated but are still extracted in the same kicker time window as shown in Figure 1b. Thus, the extracted beam from R3 still includes both the ground and isomeric states, which are tagged by their revolution times, precisely measured with the conventional mass measurement technique. An example of an isomer in ^{128m}Sn is shown in Ref. [54]. Two peaks corresponding to the ground and isomeric states in ^{128}Sn were observed with a time of flight difference of $\sim$13 ns.

3.1.3. Isomer Filter Mode

In a case that storage times can be extended to more than 10 ms, pure isomer beams will be realized. As shown in Figure 1c, the longer the storage time, the larger the time separation between the ground and isomeric states, even if the mass difference is tiny. Eventually, the isomer will be on the opposite side along the storage orbit relative to the ground state. Then, the kicker magnetic field with a flat-top of 100 ns can be adjusted to eject the isomer only, where the time difference matches half of the revolution time, approximately 180 ns. This will enable a pure isomer beam after R3. Following the expression introduced in Section 3.1.2, as an example, a storage of 20 ms is required to separate an

isomer ^{79m}Zn ($E_x = 942(10)$ keV, $T_{1/2} > 200$ ms) from the ground state at beam energy of 180 MeV/nucleon. The details of feasibility studies will be published elsewhere [55].

R3 exploits the time differences of mass doublets under the isochronous condition, whereas ESR takes advantage of the spacial differences of cooled beams, as described below. Both tiny differences caused by the mass difference between the ground and isomeric states are fully controlled by the storage-ring technologies.

3.2. Long-Lived Isomers at ESR

For long-lived nuclei, the Experimental Storage Ring (ESR) at GSI/FAIR will be available to produce isomer beams making use of the beam manipulation techniques. Figure 2 shows a part of the beamline layout at GSI/FAIR.

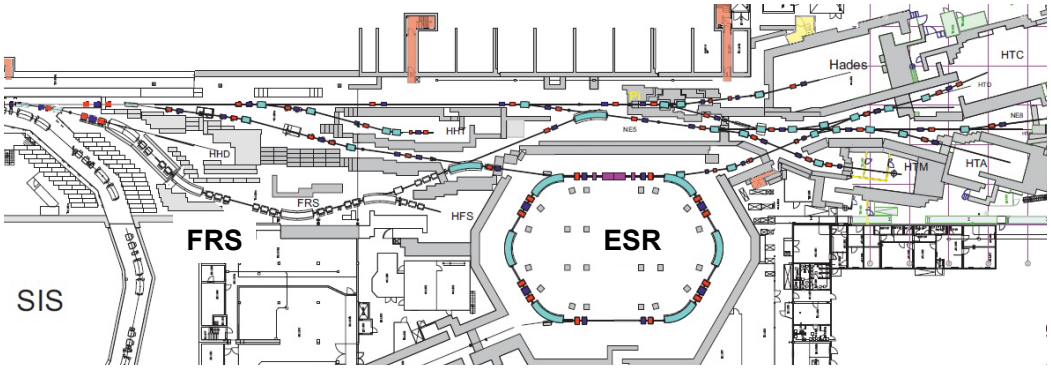


Figure 2. The high-energy beamline layout at GSI/FAIR. Radioactive ion beams produced at FRS are accumulated in ESR through the cooling and stacking techniques. Scrapers select a single species from the cocktail beam, which is extracted as a pure beam to an external cave (e.g., HTA) via charge exchange process.

The SIS synchrotron can accelerate all the stable ions from hydrogen to uranium up to magnetic rigidity of 18 Tm, corresponding to more than 1 GeV/nucleon for uranium. The extracted bunched beam is utilized to irradiate a production target, typically a plate of beryllium, in front of FRS, where projectile fragmentation or in-flight fission reaction is used to produce secondary radioactive beams. These are in-flight separated with the standard $B\rho - \Delta E - B\rho$ technique in FRS and injected into ESR. Note, that radioactive ion beams from FRS are also bunched, meaning that various ion species including isomers are compacted in time and space. To produce isomer beams at ESR, the following procedure is proposed:

- Production of radioactive ion beams at FRS;
- Accumulation with the cooling and stacking techniques at ESR;
- Cooling of the beam on the central orbit;
- Scraping to purify a single species, an isomer;
- Extraction to an external cave, e.g., by using charge pickup process.

Because target isomers are rather long-lived, the beam accumulation technique is applicable for smaller yields and/or smaller isomer ratios. Injected ions are first cooled by the stochastic and electron cooling technique and then they are moved to an inner orbit to form a stack. The next beam is injected on the outer orbits without affecting the stack. Several cycles are repeated until a sufficient intensity is reached in the ring. For instance, in the ^{205}Tl experiment [18], more than 100 cycles were possible. The stochastic cooling requires a fixed beam energy of 400 MeV/nucleon, which realizes fast cooling. The Schottky detectors non-destructively observe the revolution frequencies of stored ions, which are proportional to their mass-to-charge ratios; precision particle identification in the ring. Note, that the mass resolving power depends on the number of stored ions [48].

Although the mass differences between ground and isomeric states are small, well-cooled beams follow spatially different orbits at dispersive points along the ring circumference. This may allow us to mechanically separate the isomer from the ground state. Figure 3 illustrates an example of Schottky spectrogram of the electron capture (EC) decay of $^{140}Pr^{58+}$ to $^{140}Ce^{58+}$ to demonstrate such a scraping technique [56,57]. The EC parent and daughter nuclei have the same A/Q with a small mass difference of Q_{EC} value ($Q_{EC} \approx 3.4\,\mathrm{MeV}$, $\frac{\Delta m}{m} \approx 2.57 \times 10^{-5}$), which are well separated in frequency as shown in Figure 3 (left). One of the fine-controlled scrapers was inserted into the parent orbit and successfully purified the beam such that only the daughter ions were revolving in the ring (Figure 3, right). Here, the spatial difference, Δx, at the scraper position is calculated to be $\Delta x = D\frac{\Delta m}{m} \approx 26\ \mu\mathrm{m}$, where the dispersion is assumed to be $D = 1$ m. See Ref. [56] for more details. This technique will be available for isomer–ground doublets, making the production of pure isomer beams feasible. One example of the production of a pure beam of ^{129}Sb isomers is discussed in the context of the search for elusive process of nuclear excitation by electron capture [3].

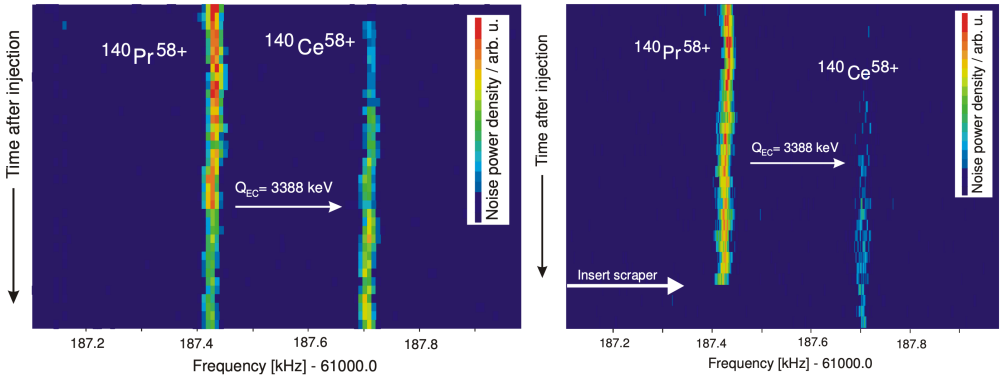


Figure 3. An example of the EC decay of $^{140}Pr^{58+}$ to $^{140}Ce^{58+}$ at ESR, reproduced from [56]. The horizontal axis represents revolution frequency and the vertical one represents time after injection. (**Left**) Two lines from top to bottom correspond to the decay of parent and the growth of daughter ions, both well separated by the Q_{EC}-value. (**Right**) The same as left but a scraper fine-controlled inserted to remove the parent $^{140}Pr^{58+}$. The frequency difference between $^{140}Pr^{58+}$ and $^{140}Ce^{58+}$ corresponds to the spatial displacement of 26 μm.

One well controlled way to extract the isomers from the ring is to utilize atomic charge pickup process at the ESR cooler. If an ion from the stored isomer beam captures an electron at the cooler, the magnetic rigidity suddenly becomes larger and the orbit jumps to an outer side leading to an extraction septum magnet. This technique has been already successfully demonstrated at the resonant coherent excitation experiment of U^{89+} beam [58]. The extracted beam was available at an external cave (HTA shown in Figure 2). The intensities of isomer beams greatly depend on the isomer ratios of the target nucleus and the extraction efficiency, which will be tested in the coming years [59].

3.3. Present Technical Limitations of Isomer Beam Production

Currently, some technical limitations prevent efficient preparation of isomer beams. In general, isomer production ratios depend on underlying reaction mechanisms, ranging from a few % up to 30–40%. See Refs. [60,61] for example. For R3, the kicker can currently be used with a repetition frequency of 100 Hz at maximum, and the efficiency from injection to extraction is a few %, which is foreseen to be upgraded via an implementation of steering magnets. Therefore, isomer beam intensities will be $\lesssim 1$ Hz. The beam energies should be less than 200 MeV/nucleon due to the individual injection scheme.

For ESR, the beam accumulation technique is applicable for small isomeric ratios. However, as described in 2.2, the mass resolving power, R, depends on the number of stored ions, n, and amounts to $R \sim 10^5$ for $n \lesssim 10^3$ [48]. Therefore, isomer beam intensities will be $\lesssim 10^3$ particles/cycle. The beam intensities and resolving power need to be optimized on a case-by-case basis. The beam energies are limited to less than 420 MeV/nucleon due to the maximum voltage of electron cooler.

4. Physics Cases

Isomers have been studied with the γ-ray spectroscopy technique. The present isomer beam technique is complementary and will realize direct reaction studies to investigate isomer structures, where many strongly-deformed and high-spin states exist, thus opening a new opportunity for radioactive ion beam experiments.

The first envisioned experiments can be total reaction and charge-changing cross section measurements, which are feasible even for low intensities of isomer beams. A thick target can be used to compensate for low luminosities. The reaction cross sections are a good probe of matter radii, whereas charge changing cross sections are sensitive to point-proton radii. Both cross sections allow one to separate neutron and proton components from matter radii, giving a stringent test of nuclear wavefunction calculations. Higher intensities in the future will further make proton elastic scattering experiments possible.

One of the intriguing physics cases relates to Hf isotopes. The charge radii of the isomeric and ground states were measured by laser spectroscopy [62]. Surprisingly, the charge radius of the isomer in ^{178}Hf is smaller than the one of the ground state, despite a larger quadrupole deformation observed. No successful theoretical explanation exists till now. There are further similar cases reported, where cross section data can provide additional information to their structures.

5. Summary

This article proposes the isomer beam production technique using ion storage rings. For short-lived isomers, the Rare-RI Ring facility at RIBF will be available, where storage time differences are utilized to separate isomers from the ground states. For longer-lived isomers, the ESR facility at GSI/FAIR will be employed, where the separation via distinct storage orbits is implemented. Consequently, tagged or pure isomer beams covering a wide range of lifetimes will be available in laboratories. This will enable direct reactions to probe the different structures between the ground and excited states. Even with low intensities, reaction cross sections of isomers will currently be measured using a thick external target, much like the discovery of the halo structure 40 years ago. The feasibility studies with beam will be conducted at RIBF and GSI/FAIR in the near future.

Author Contributions: Conceptualization, T.Y. and Y.Y.; methodology, T.Y. and Y.A.L.; writing—original draft preparation, T.Y.; writing—review and editing, Y.Y., T.O., D.N. and Y.A.L.; project administration, T.Y.; funding acquisition, T.Y. All authors have read and agreed to the published version of the manuscript.

Funding: The present work was partly supported by JSPS KAKENHI Grant Numbers 21H04461.

Institutional Review Board Statement: Not applicable.

Informed Consent Statement: Not applicable.

Data Availability Statement: Data are available upon reasonable request.

Acknowledgments: The present work was partly supported by collaborators in the international Isomeric Beams, LIfetimes and MAsses (ILIMA) collaboration at GSI/FAIR and the Rare-RI Ring (R3) collaboration at RIBF.

Conflicts of Interest: The authors declare no conflicts of interest.

References

1. Steck, M.; Litvinov, Y.A. Heavy-ion storage rings and their use in precision experiments with highly charged ions. *Prog. Part. Nucl. Phys.* **2020**, *115*, 103811. [CrossRef]
2. Franzke, B. The heavy ion storage and cooler ring project ESR at GSI. *Nucl. Instrum. Meth. Phys. Res. B* **1987**, *24/25* , 18. [CrossRef]
3. Lestinsky, M.; Andrianov, V.; Aurand, B.; Bagnoud, V.; Bernhardt, D.; Beyer, H.; Bishop, S.; Blaum, K.; Bleile, A.; Borovik, A., Jr.; et al. Physics book: CRYRING@ESR. *Eur Phys. J. Spec. Top.* **2016**, *225*, 797. [CrossRef]
4. Xia, J.W.; Zhan, W.L.; Wei, B.W.; Yuan, Y.J.; Song, M.T.; Zhang, W.Z.; Yang, X.D.; Yuan, P.; Gao, D.Q.; Zhao, H.W.; et al. The heavy ion cooler-storage-ring project (HIRFL-CSR) at Lanzhou. *Nucl. Instrum. Meth. Phys. Res. A* **2002**, *488*, 11. [CrossRef]
5. Ozawa, A.; Uesaka, T.; Wakasugi, M. The rare-RI ring. *Prog. Theor. Exp. Phys.* **2012**, 2012, 03C009. [CrossRef]
6. Wu, B.; Yang, J.C.; Xia, J.W.; Yan, X.L.; Hu, X.J.; Mao, L.J.; Sheng, L.N.; Wu, J.X.; Yin, D.Y.; Chai, W.P.; et al. The design of the Spectrometer Ring at the HIAF. *Nucl. Instrum. Meth. Phys. Res. B* **2018**, *881*, 27. [CrossRef]
7. Yang, J.C.; Xia, J.W.; Xiao, G.Q.; Xu, H.S.; Zhao, H.W.; Zhou, X.H.; Ma, X.W.; He, Y.; Ma, L.Z.; Gao, D.Q.; et al. High Intensity heavy ion Accelerator Facility (HIAF) in China. *Nucl. Instrum. Meth. Phys. Res. B* **2013**, *317*, 263. [CrossRef]
8. Yamaguchi, T.; Koura, H.; Litvinov, Y.A.; Wang. M. Masses of exotic nuclei. *Prog. Part. Nucl. Phys.* **2021**, *120*, 103882. [CrossRef]
9. Franzke, B.; Geissel, H.; Münzenberg, G. Mass and lifetime measurements of exotic nuclei in storage rings. *Mass Spectro. Rev.* **2007**, *27*, 428. [CrossRef]
10. Möhl, D. Stochastic Cooling of Particle Beams. *Lect. Notes Phys.* **2013**, *866*, 1.
11. Poth, H. Electron cooling: Theory, experiment, application. *Phys. Rep.* **1990**, *196*, 135. [CrossRef]
12. Litvinov, Y.A.; Geissel, H.; Novikov, Y.N.; Patyk, Z.; Radon, T.; Scheidenberger, C.; Attallah, F.; Beckert, K.; Bosch, F.; Falch, M.; et al. Precision experiments with time-resolved Schottky mass spectrometry. *Nucl. Phys. A* **2004**, *734*, 473. [CrossRef]
13. Litvinov, Y.A.; Geissel, H.; Radon, T.; Attallah, F.; Audi, G.; Beckert, K.; Bosch, F.; Falch, M.; Franzke, B.; Hausmann, M.; et al. Mass measurement of cooled neutron-deficient bismuth projectile fragments with time-resolved Schottky mass spectrometry at the FRS-ESR facility. *Nucl. Phys. A* **2005**, *756*, 3. [CrossRef]
14. Nolden, F.; Hülsmann, P.; Litvinov, Y.A.; Moritz, P.; Peschke, C.; Petri, P.; Sanjari, M.S.; Steck, M.; Weick, H.; Wu, J.X.; et al. A fast and sensitive resonant Schottky pick-up for heavy ion storage rings. *Nucl. Instrum. Meth. Phys. Res. A* **2011**, *659*, 69. [CrossRef]
15. Sanjari, M.S.; Dmytriiev, D.; Litvinov, Y.A.; Gumenyuk, O.; Hess, R.; Joseph, R.; Litvinov, S.A.; Steck, M.; Stöhlker, T. A 410 MHz resonant cavity pickup for heavy ion storage rings. *Rev. Sci. Instrum.* **2020**, *91*, 083303. [CrossRef] [PubMed]
16. Litvinov, Y.A.; Bosch, F. Beta decay of highly charged ions. *Rep. Prog. Phys.* **2011**, *74*, 016301. [CrossRef]
17. Litvinov, Y.A.; Chen, R.J. Radioactive decays of stored highly charged ions. *Eur. Phys. J. A* **2023**, *59*, 102. [CrossRef]
18. Leckenby, G.; Sidhu, R.S.; Chen, R.J.; Mancino, R.; Szányi, B.; Bai, M.; Battino, U.; Blaum, K.; Brandau, C.; Cristallo, S.; et al. High-temperature ^{205}Tl decay clarifies ^{205}Pb dating in early Solar System. *Nature* **2024**, *635*, 321. [CrossRef]
19. Sidhu, R.S.; Leckenby, G.; Chen, R.J.; Mancino, R.; Neff, T.; Litvinov, Y.A.; Martínez-Pinedo, G.; Amthauer, G.; Bai, M.; Blaum, K.; et al. Bound-state beta decay of ^{205}Tl^{81+} ions and the LOREX project. *Phys. Rev. Lett.* **2024**, *133*, 232701. [CrossRef]
20. Suzuki, S.; Ozawa, A.; Kamioka, D.; Abe, Y.; Amano, M.; Arakawa, H.; Ge, Z.; Hiraishi, K.; Ichikawa, Y.; Inomata, K.; et al. Efficiency and timing performance of time-of-flight detector utilizing thin foils and crossed static electric and magnetic fields for mass measurements with Rare-RI Ring facility. *Nucl. Instrum. Meth. Phys. Res. A* **2020**, *965*, 163807. [CrossRef]
21. Wang, M.; Zhang, M.; Zhou, X.; Zhang, Y.H.; Litvinov, Y.A.; Xu, H.S.; Chen, R.J.; Deng, H.Y.; Fu, C.Y.; Ge, W.W.; et al. $B\rho$-defined isochronous mass spectrometry: An approach for high-precision mass measurements of short-lived nuclei. *Phys. Rev. C* **2022**, *106*, L501301. [CrossRef]
22. Zhou, X.; Wang, M.; Zhang, Y.H.; Litvinov, Y.A.; Meisel, Z.; Blaum, K.; Zhou, X.H.; Hou, S.Q.; Li, K.A.; Xu, H.S.; et al. Mass measurements show slowdown of rapid proton capture process at waiting-point nucleus ^{64}Ge. *Nat. Phys.* **2023**, *19*, 1091. [CrossRef]
23. Xing, Y.M.; Luo, Y.F.; Zhang, Y.H.; Wang, M.; Zhou, X.H.; Li, J.G.; Li, K.H.; Yuan, Q.; Niu, Y.F.; Guo, J.Y.; et al. Z = 14 Magicity Revealed by the Mass of the Proton Dripline Nucleus ^{22}Si. *Phys. Rev. Lett.* **2025**, *135*, 012501. [CrossRef] [PubMed]
24. Glorius, J.; Langer, C.; Slavkovská, Z.; Bott, L.; Brandau, C.; Brückner, B.; Blaum, K.; Chen, X.; Dababneh, S.; Davinson, T.; et al. Approaching the Gamow window with stored ions: Direct measurement of ^{124}Xe(p,γ) in the ESR storage ring. *Phys. Rev. Lett.* **2019**, *122*, 092701. [CrossRef]
25. Varga, L.; Glorius, J.; Aliotta, M.; Blaum, K.; Bott, L.; Brandau, C.; Brückner, B.; Bruno, C.G.; Chen, X.; Chen, R.; et al. Nuclear Astrophysics in the Storage Ring: Background Suppressed Simultaneous Measurement of (p,γ) and (p,n) Reactions. *Phys. Rev. Lett.* **2025**, *134*, 082701. [CrossRef]
26. Sguazzin, M.; Jurado, B.; Pibernat, J.; Swartz, J.A.; Grieser, M.; Glorius, J.; Litvinov, Y.A.; Adamczewski-Musch, J.; Alfaurt, P.; Ascher, P.; et al. First measurement of the neutron-emission probability with a surrogate reaction in inverse kinematics at a heavy-ion storage ring. *Phys. Rev. Lett.* **2025**, *134*, 072501. [CrossRef]

27. Sguazzin, M.; Jurado, B.; Pibernat, J.; Swartz, J.A.; Grieser, M.; Glorius, J.; Litvinov, Y.A.; Berthelot, C.; Włoch, B.; Adamczewski-Musch, J.; et al. First simultaneous measurement of the γ-ray and neutron emission probabilities in inverse kinematics at a heavy-ion storage ring. *Phys. Rev. C* **2025**, *111*, 024614. [CrossRef]
28. Grigoryev, K. Internal targets at storage rings. *Phys. Scripta* **2015**, *T166*, 014050. [CrossRef]
29. Glorius, J.; Litvinov, Y.A.; Aliotta, M.; Amjad, F.; Brückner, B.; Bruno, C.G.; Chen, R.; Davinson, T.; Dellmann, S.F.; Dickel, T.; et al. Storage, accumulation and deceleration of secondary beams for nuclear astrophysics. *Nucl. Instrum. Meth. Phys. Res. B* **2023**, *541*, 190. [CrossRef]
30. Dellmann, S.; Glorius, J.; Litvinov, Y.A.; Reifarth, R.; Varga, L.; Aliotta, M.; Amjad, F.; Blaum, K.; Bott, L.; Brandau, C.; et al. First proton-induced cross sections on a stored rare ion beam: Measurement of ^{118}Te(p, γ) for explosive nucleosynthesis. *Phys. Rev. Lett.* **2025**, *134*, 142701. [CrossRef]
31. Geissel, H.; Armbruster, P.; Behr, K.H.; Brünle, A.; Burkard, K.; Chen, M.; Folger, H.; Franczak, B.; Keller, H.; Klepper, O.; et al. The GSI projectile fragment separator (FRS): A versatile magnetic system for relativistic heavy ions. *Nucl. Instrum. Meth. Phys. Res. B* **1992**, *70*, 286. [CrossRef]
32. Burno, C.G.; Marsh, J.J.; Davinson, T.; Woods, P.J.; Black, P.; Bräuning-Demian, A.; Glorius, J.; Grant, A.; Hall, O.; Headspith, A.; et al. CARME—The CRYRING array for reaction measurements A new approach to study nuclear reactions using storage rings. *Nucl. Instrum. Meth. Phys. Res. A* **2023**, *1048*, 168007. [CrossRef]
33. Marsh, J.; Bruno, C.G.; Davinson, T.; Woods, P.J.; Andelkovic, Z.; Bräuning-Demian, A.; Chen, R.J.; Dellmann, S.F.; Erbacher, P.; Fedotova, S.; et al. The first in-beam reaction measurement at CRYRING@ESR using the CARME array. *Eur. Phys. J. A* **2024**, *60*, 95. [CrossRef]
34. Marsh, J.; Bruno, C.G.; Davinson, T.; Woods, P.J.; Andelkovic, Z.; Barbieri, L.; Bemmerer, D.; Biniskos, A.; Boudefla, D.; Corvisiero, P.; et al. First sub-MeV nuclear reaction measurements in a heavy-ion storage ring. *Eur. Phys. J. A* **2026**, *62*, 10. [CrossRef]
35. Tanihata, I.; Hamagaki, H.; Hashimoto, O.; Nagamiya, S.; Shida, Y.; Yoshikawa, N.; Yamakawa, O.; Sugimoto, K.; Kobayashi, T.; Greiner, D.E.; et al. Measurements of interaction cross sections and radii of He isotopes. *Phys. Lett. B* **1985**, *160*, 380. [CrossRef]
36. Tanihata, I.; Hamagaki, H.; Hashimoto, O.; Shida, Y.; Yoshikawa, N.; Sugimoto, K.; Yamakawa, O.; Kobayashi, T.; Takahashi, N. Measurements of interaction cross sections and nuclear radii in the light p-shell region. *Phys. Rev. Lett.* **1985**, *55*, 2676. [CrossRef]
37. Glauber, R.J. High-energy collision theory. In *Lectures in Theoretical Physics*; Brittin, W.E., Dunham, L.G., Eds.; Interscience: New York, NY, USA, 1959; Volume 1, p. 315.
38. Dufour, J.P.; Del Moral, R.; Emmermann, H.; Hubert, F.; Jean, D.; Poinot, C.; Pravikoff, M.S.; Fleury, A.; Delagrange, H.; Schmidt, K.-H. Projectile fragments isotopic separation: Application to the LISE spectrometer at GANIL. *Nucl. Instrum. Methods Phys. Res. A* **1986**, *248*, 267. [CrossRef]
39. Morrissey, D.J.; Sherrill, B.M.; Steiner, M.; Stolz, A.; Wiedenhoever, I. Commissioning the A1900 projectile fragment separator. *Nucl. Instrum. Meth. Phys. Res. B* **2003**, *204*, 90. [CrossRef]
40. Xu, X.D.; Zheng, Y.; Sun, Z.Y.; Song, Y.N.; Sun, B.H.; Terashima, S.; Wang, C.J.; Guo, G.; Li, G.S.; Wei, X.L.; et al. Full realization of the RIBLL2 separator at the HIRFL-CSR facility. *Sci. Bull.* **2025**, *70*, 1026. [CrossRef]
41. Kubo, T. In-flight RI beam separator BigRIPS at RIKEN and elsewhere in Japan. *Nucl. Instrum. Meth. Phys. Res. B* **2003**, *204*, 97. [CrossRef]
42. Portillo, M.; Sherrill, B.M.; Choi, Y.; Cortesi, M.; Fukushima, K.; Hausmann, M.; Kwan, E.; Lidia, S.; Ostroumov, P.N.; Ringle, R.; et al. Commissioning of the advanced rare isotope separator ARIS at FRIB. *Nucl. Instrum. Meth. Phys. Res. B* **2023**, *540*, 151. [CrossRef]
43. Sheng, L.N.; Zhang, X.H.; Zhanga, J.Q.; Yang, J.C.; Sun, Z.Y.; Maoa, L.J.; Wua, W.; Yin, D.Y.; Ruana, S.; Shen, G.D.; et al. Ion-optical design of high energy fragment separator (HFRS) at HIAF. *Nucl. Instrum. Meth. Phys. Res. B* **2020**, *469*, 1. [CrossRef]
44. Geissel, H.; Weick, H.; Winkler, M.; Münzenberg, G.; Chichkine, V.; Yavor, M.; Aumann, T.; Behr, H.H.; Böhmer, M.; Brünle, A.; et al. The Super-FRS project at GSI. *Nucl. Instrum. Meth. Phys. Res. B* **2003**, *204*, 71. [CrossRef]
45. Kubota, Y.; Corsi, A.; Authelet, G.; Baba, H.; Caesar, C.; Calvet, D.; Delbart, A.; Dozono, M.; Feng, J.; Flavigny, F.; et al. Surface localization of the dineutron in ^{11}Li. *Phys. Rev. Lett.* **2020**, *125*, 252501. [CrossRef]
46. Bosch, F.; Geissel, H.; Litvinov, Y.A.; Beckert, K.; Franzke, B.; Hausmann, M.; Kerscher, T.; Klepper, O.; Kozhuharov, C.; Löbner, K.E.G.; et al. Experiments with stored exotic nuclei at relativistic energies. *Int. J. Mass Spectrom.* **2006**, *251*, 212. [CrossRef]
47. Bosch, F.; Litvinov, Y.A.; Stöhlker, T. Nuclear physics with unstable ions at storage rings. *Prog. Part. Nucl. Phys.* **2013**, *73*, 84. [CrossRef]
48. Steck, M.; Beckert, K.; Eickhoff, H.; Franzke, B.; Nolden, F.; Reich, H.; Schlitt, B.; Winkler, T. Anomalous temperature reduction of electron-cooled heavy ion beams in the storage ring ESR. *Phys. Rev. Lett.* **1996**, *77*, 3803. [CrossRef]
49. Freire-Fernández, D.; Korten, W.; Chen, R.J.; Litvinov, S.; Litvinov, Y.A.; Sanjari, M.S.; Weick, H.; Akinci, F.C.; Albers, H.M.; Armstrong, M.; et al. Measurement of the isolated nuclear two-photon decay in ^{72}Ge. *Phys. Rev. Lett.* **2024**, *33*, 022502. [CrossRef]
50. Yamaguchi, T.; Yamaguchi, Y. Present and future of the Rare-RI Ring facility at RIBF. *Chin. Phys. C* **2025**, *49*, 114003. [CrossRef]

51. Nagae, D.; Omika, S.; Abe, Y.; Yamaguchi, Y.; Suzaki, F.; Wakayama, K.; Tadano, N.; Igosawa, R.; Inomata, K.; Arakawa, H.; et al. Isochronous mass spectrometry at the RIKEN Rare-RI Ring facility. *Phys. Rev. C* **2024**, *110*, 014310. [CrossRef]
52. Li, H.F.; Naimi, S.; Sprouse, T.M.; Mumpower, M.R.; Abe, Y.; Yamaguchi, Y.; Nagae, D.; Suzaki, F.; Wakasugi, M.; Arakawa, H.; et al. First Application of Mass Measurements with the Rare-RI Ring Reveals the Solar r-Process Abundance Trend at $A = 122$ and $A = 123$. *Phys. Rev. Lett.* **2022**, *128*, 152701. [CrossRef] [PubMed]
53. Abe, Y.; Yamaguchi, Y.; Wakasugi, M.; Baba, H.; Fujinawa, T.; Ge, Z.; Goto, A.; Michimasa, S.; Miura, H.; Moriguchi, T.; et al. Performance of a precise isochronous magnetic field over a wide momentum range in the Rare-RI Ring. *Nucl. Instrum. Meth. Phys. Res. A* **2025**, *1072*, 170083. [CrossRef]
54. Li, H.F.; Naimi, S.; Nagae, D.; Abe, Y.; Suzaki, F.; Yamaguchi, Y.; Wakasugi, M.; Omika, S.; Onomata, K.; Arakawa, H.; et al. Isomeric-to-ground state ratio of ^{128}Sn measured by Rare RI Ring. *RIKEN Accel. Prog. Rep.* **2020**, *53*, 48.
55. Yamaguchi, Y.; Ohnishi, T.; Yamaguchi, T.; Ozawa, A.; Yano, A.; Nagae, D.; Moriguchi, T.; Abe, Y. Rare-RI Ring as an isomer beam filter mode. *Nucl. Instrum. Meth. Phys. Res. B* in preparation.
56. Scheidenberger, C.; Beckert, K.; Beller, P.; Bosch, F.; Brandau, C.; Boutin, D.; Chen, L.; Franzke, B.; Geissel, H.; Knöbel, R.; et al. Isobar separation st FRS-ESR–a development towards pure isomeric stored beams. *Hyperf. Int.* **2006**, *173*, 61. [CrossRef]
57. Walker, P.; Litvinov, Y.A.; Geissel, H. The ILIMA project at FAIR. *Int. J. Mass Spectrom.* **2013**, *349–350*, 247. [CrossRef]
58. Nakano, Y.; Ananyeva, A.; Menk, S.; Bräuning-DemianB, A.; Bräuning, H.; Kleffner, C.; Stöhlker, T.; Azuma, T. Enhancing the energy resolution of resonant coherent excitation using the cooled U^{89+} beam extracted from the ESR. *J. Phys. Conf. Ser.* **2015**, *635*, 032016. [CrossRef]
59. Yamaguchi, T.; Blaum, K.; Chen, R.J.; Dillmann, I.; Dozono, M.; Ebata, S.; Gernhäuser, R.; Glorius, J.; Griffin, C.J.; Hess, R.; et al. Isomer beam production and its reaction studies with ESR. *GSI proposal* **2024**, unpublished.
60. Bowry, M.; Podolyäk, Z.; Pietri, S.; Kurcewicz, J.; Bunce, M.; Regan, P.H.; Farinon, F.; Geissel, H.; Nociforo, C.; Prochazka, A.; et al. Population of high-spin isomeric states following fragmentation of ^{238}U. *Phys. Rev. C* **2013**, *88*, 024611. [CrossRef]
61. Tu, X.L.; Kelić-Heil, A.; Litvinov, Y.A.; Podolyák, Z.; Zhang, Y.H.; Huang, W.J.; Xu, H.S.; Blaum, K.; Bosch, F.; Chen, R.J.; et al. Application of isochronous mass spectrometry for the study of angular momentum population in projectile fragmentation reactions. *Phys. Rev. C* **2017**, *95*, 014610. [CrossRef]
62. Bissell, M.L.; Flanagan, K.T.; Gardner, M.D.; Avgoulea, M.; Billowes, J.; Campbell, P.; Cheal, B.; Eronen, T.; Forest, D.H.; Huikari, J.; et al. On the decrease in charge radii of multi-quasi particle isomers. *Phys. Lett. B* **2007**, *645*, 330. [CrossRef]

Disclaimer/Publisher's Note: The statements, opinions and data contained in all publications are solely those of the individual author(s) and contributor(s) and not of MDPI and/or the editor(s). MDPI and/or the editor(s) disclaim responsibility for any injury to people or property resulting from any ideas, methods, instructions or products referred to in the content.